

ORIGINAL RESEARCH PAPER

Removal of Malathion on Carbon using Iron Oxide Nanoparticles (Fe_3O_4) in Aquatic Environments

Malektaj Eskandari makvand^{1*}, Sima Sabzalipour¹, Mahboobeh Cheraghi¹, Neda Orak¹

1. Department of Environment, Ahvaz Branch, Islamic Azad University, Ahvaz, Iran

*Correspondence author: malektaj.eskandarimakvand@yahoo.com

Received: 25 April 2021/ Accepted: 13 August 2021/ Published: 15 September 2021

Abstract: The development of nanotechnology and the possible entry of nanoparticles into aquatic environments have raised environmental concerns. The present study aimed to investigate the effect of iron oxide nanoparticles (Fe_3O_4) loaded on carbon to remove malathion in order to evaluate the toxicity potential of nanoparticles in aqueous environments. We examined the characteristics of iron oxide nanoparticles (Fe_3O_4) using XRD refraction, Fourier irradiated spectroscopy (FTIR), the catalytic activity of iron nanoparticles for activation of persulfate, and malathion decomposition. Moreover, we assessed the influence of effective parameters on this process, such as pH, persulfate concentration, and the number of iron oxide nanoparticles (Fe_3O_4). The results showed that 82% of malathion was decomposed by the combined process of iron oxide nanoparticles loaded on carbon at pH = 5 and 0.4 g of iron nanoparticles in 60 minutes. Additionally, according to the results obtained from the advanced oxidation processes, it able to optimally remove malathion from the aquatic environment. This study revealed that nanoparticle stabilization technology on activated carbon could be used as an effective, efficient, and fast adsorbent to remove certain contaminants, such as malathion, from aqueous solutions. Although the combination of processes may complicate their analysis and mechanism, the study of this process could be a promising emergence of hybrid processes in water and wastewater treatment. In general, the results of this study relatively indicated that the physicochemical properties of nanoparticles, such as size, shape, surface, general morphology, and chemical composition, in different environmental conditions can significantly affect carbon in removing the malathion.

Keywords: Nanotechnology, Aqueous environment, Carbon, Iron oxide, Removal of malathion



This work is licensed under the Creative Commons Attribution 4.0 International License. To view a copy of this license, visit <http://creativecommons.org/licenses/by/4.0/>.

Introduction

Wastewater disposal from industrial section is known as a major problem in most countries around the world (Venkatesan and Subramani, 2018). It strongly affects surface water and groundwater (Edokpayi et al., 2017; Fataei et al., 2013; Sasani et al., 2021).

The release of toxic substances into the environment can have adverse effects on humans and other living organisms (Zhang et al., 2020; Omrani and Fataei, 2018). Contamination due to the accumulation of toxic substances in soil causes diseases with detrimental effects on the growth and health of animals and humans (Li et al., 2019). Currently, one of the pollutions faced by the environment is the presence of resistant organic compounds in the wastewater of chemical industries and agricultural effluents (Schwarzenbach et al., 2010). The presence of these compounds in aquatic environments can change the chemical quality, chemical oxygen demand, alkalinity, acidity, dissolved oxygen, and physical quality of water (Nogueira et al., 2020). Nanoparticles are

currently made from a wide range of materials, mostly ceramic, metal, and polymer (Khalili Arjaghi et al., 2020). They are used in various industries (Rajaei et al., 2020). Some of these nanoparticles are discharged into the environment from industrial wastewater or other industrial wastes, such as solid waste. These depleted nanoparticles may have detrimental environmental effects (Saravanan et al., 2021). The rate of production and application of nanoparticles has increased and as a result, the rate of environmental and human exposure has also been on an increasing trend (Khan et al., 2019). It has been indicated that nanoparticles can have adverse effects on a variety of environmental ecosystems (Arjaghi et al., 2021). It has previously been reported that nanoparticles could be absorbed by human and animal blood and move through the blood to other organs and tissues, such as liver, heart, and blood cells (Nowach, 2009). In studies like that by Safarkar et al. (2020), it was pointed that some of nanoparticles (like iron oxide) are not only non-toxic to

the human body at low concentrations, but also are a good alternative to antibiotics. These substances inhibit bacterial growth at lower concentrations compared with antibiotics and have much fewer side effects.

Studies on nanoparticle toxicity are still incomplete. Information on the behavior and toxicity of nanoparticles has mainly emerged from studies on nanoparticles inhaled on lung tissue. However, nanoparticles can have different effects on different organisms depending on their size, shape, solubility, chemical composition, and specific surface activity (Buchman et al., 2020). Numerous studies have indicated that many physicochemical properties of nanoparticles, such as size distribution, shape, surface area, electrostatic particles, morphology, chemical composition, physicochemical stability, crystal structure, surface energy, and aggregation may significantly contribute to toxicity in the environment regarding these nanomaterials (Sengul and Asmatulu, 2020). With the widespread production of Nano-centric products, it is highly essential to investigate their potential toxic effects on the human body and the environment (Paramo et al., 2020). Environmental factors may play a role in the toxicity of iron oxide nanoparticles. Climatic conditions, such as humidity, temperature, wind speed, and altitude, could affect certain properties of nanoparticles that cause toxicity (Zhang et al., 2020). Aquatic environments are also affected by contaminated nanoparticles, like Fe_3O_4 (Peng et al., 2017). They are toxic to aquatic animals, for instance, fish and single-celled organisms. The study of the interaction between iron oxide nanoparticles and soil environment is of great importance, through which we could understand the existing interactions (Ray et al., 2018). According to the existing literature review, several studies have been conducted on the effect of nanoparticles in *In Vitro* and *In Vivo* systems (Bacchetta et al., 2017). Khalili Arjaghi et al. (2020) studied the removal of mercury and arsenic metal pollutants from water using iron oxide nanoparticles synthesized from lichen *sinensis* Ramalina extract. In the study by Rezaei Aghdam et al. (2021), TiO_2 , ZnO , and CTAB-stabilized Fe_3O_4 nanocomposite were successfully synthesized and employed for the removal of yellow 145 dye from aqueous solutions. Liu et al. (2019) studied enhanced dyes adsorption from wastewater via Fe_3O_4 nanoparticles functionalized activated carbon. It is necessary to develop a cost-effective, sensitive, and rapid assay method for evaluating the toxicity of nanoparticles in aqueous environments (Bownik et al., 2017). Cobalt oxide and iron oxide are converted into particles less than 100 nanometers, which are called nanoparticles, using nanotechnology (Gajda and Meissner et al., 2020). However, these materials may enter the water cycle during manufacturing and application and are hazardous to aquatic life. The severity of these hazards depends on several factors, such as size, type of nanoparticles, charge, and aquatic species exposed to them (Zhou et al., 2017). Today, the increasing need for food has led to the

expansion of agriculture and the consequent increase in the use of water and agriculture-associated chemical products (Deknock et al., 2019). Among the types of pesticides, the compound $\text{C}_{10}\text{H}_{19}\text{O}_6\text{PS}_2$ (Malathion) is widely utilized in agriculture and home and is produced by more than hundreds of commercial species in the world. It is used in all countries with a different production rate of wheat and cereals. This pesticide is also employed selectively and non-selectively for a variety of plants owing to its high efficiency in killing weeds (Köck-Schulmeyer et al., 2013). The presence of this substance in soil and surface water and groundwater has caused many concerns (Vymazal and Březinová, 2015; Guan et al., 2013). Numerous treatment methods have been proposed for the treatment of malathion. Among the treatment methods, chemical oxidation processes have attracted a great deal of attention owing to their high efficiency in mineralization and detoxification (Tony et al., 2017). In advanced oxidation processes, a chemical oxidant is often used to produce and activate double-activated radicals to remove organic compounds. There are several methods for generating hydroxyl radicals, including chemical, photochemical, and electrochemical processes (Olaniran et al., 2017; Asghar et al., 2015).

Iron residues should be separated into homogeneous 2 and 3 valent forms using solvents that require further processing. However, inhomogeneous catalysis can be reused, which is a significant advantage compared to the homogeneous form of this material (Zhu et al., 2013). In addition, Fe_3O_4 has shown good stability in the photo catalysis process (Mishra and Chun, 2015). The present study was conducted to analyze the catalytic effects of Fe_3O_4 on the degradation of malathion and iron oxide nanoparticles (Fe_3O_4).

Materials and Methods

a. Raw Material

The number of samples in the experiment was 246 and the method was modeled on the book named "APHA, Standard Methods for the Examination of Water and Wastewater. 22th. Washington DC. APHA (2012)". The initial materials used in the experiment were malathion (98% pure), persulfate salt, sodium persulfate, hydrochloric acid, chlorine iron purchased from the German Merck factory, Ferrous sulfate purchased from Sigma America factory, injector filter from Comlab, Belgium factory persulfate salt purchased from Petrochimia factory in Iran, iron oxide nanoparticle (Fe_3O_4) from ArminaCo factory in Iran, iron chloride (FeCl_3) purchased from TomadKala Co.

b. Experimental Process

To synthesize magnetic iron oxide nanoparticles (Fe_3O_4), the first 0.1 g of vitamin C was mixed with two solutions of iron chloride, quaternary divalent iron chloride, and hexavalent trivalent iron chloride in a ratio of 1 to 2. The role of vitamin C was to inhibit divalent iron oxidation during the reaction. The resulting solution was stirred for 10 to 15 minutes. Afterwards, the pH of the

solution was raised to 10, using ammonia solution. The resulting solution was then placed at 80 ° C for 30 to 40 minutes. Synthesis of Fe₃O₄ nanoparticles was obtained through the reaction in Equation (1) (Teja and Koh, 2009). $\text{Fe}^{2+} + 2\text{Fe}^{3+} + 8\text{OH}^- \longrightarrow \text{Fe}_3\text{O}_4 + 4\text{H}_2\text{O}$ (1)

The resulting precipitates were washed with distilled water and ethanol and placed in an oven at 60 ° C for 10 hours and Fe₃O₄ @ CNT nanocomposite with a concentration of 10⁻² × 6.25 g/L was obtained. X-Ray Diffraction (XRD) made by Burker.Co, model D8 advance was employed to determine the X-ray scattering pattern and the presence of Fe and Magnetite particles in the catalyst structure. Finally, EDX analysis method was used to determine the ratio of elements in the catalyst structure (Slater et al., 2016). The surface and morphological characteristics of the catalyst were also investigated via SEM analysis.

At this stage, the efficiency of the synthesized nanocomposite in removing malathion from aqueous solutions was determined by one factor at a time. After determining the optimal ratio of carbon nanotubes to iron in three levels of iron with carbon nanotubes of 0.25, 0.5, and 1, based on the malathion removal efficiency, the effect of each variable was investigated as follows: the studied variable factors included pH in the range of 3 to 11 (3, 5, 7, 9, and 11), values of different concentrations of catalyst (MNP @ CNT) at five levels (0.1, 0.2, 0.3, 0.4

and 0.5 g / l), malathion concentration at eight levels (1, 5, 10, 20, 40, 60, 80 and 100 mg / l), persulfate concentration in the range of 0.5 to 2 mM (0.5, 1, 1.5 and 2 mM), TOC values (as process mineralization index), and residual iron values (as catalyst stability indicators). The process efficiency was also evaluated in the analysis of malathion by changing the values of these parameters. We investigated the effect of these parameters based on the method of one factor in variable times. This means that at each stage of the experiment, its effect was evaluated by keeping the other parameters constant and changing only one variable at different times. The reusability of the catalysts and their stability was investigated by measuring the amount of iron released into the medium under selected conditions for five consecutive use cycles. The TOC index was measured in order to assess the mineralization process. Moreover, the synthetic sample was prepared using groundwater and under the selected conditions and the malathion removal performance was evaluated by MNP @ CNT process (Figure 1). The removal efficiency was calculated via Equation (2):

$$R = (C_0 - C_t) / (C_0) \times 100\% \quad (2)$$

where R is the malathion removal efficiency, C₀ is the initial malathion concentration, and C_t is the malathion concentration at time t. Figure 1 depicts the schematic view of the studied mechanism for malathion degradation.

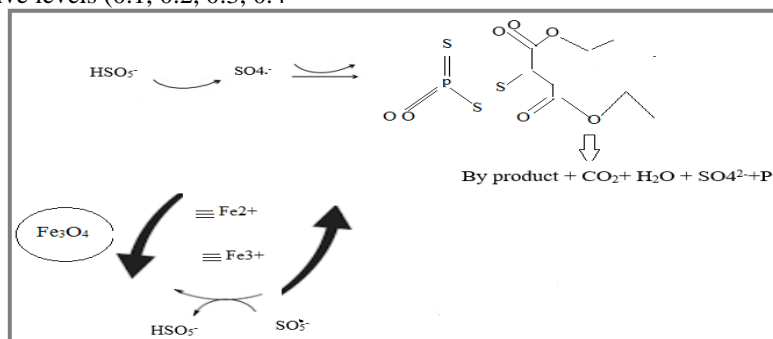


Figure.1- Schematic view of the studied mechanism for malathion degradation.

(Analytic Jena. Vario 6). All the experiments were performed at +25 ± 2 ° C.

c. Methods of Diagnosis and Measurement

The mobile phase also contained a mixture of HPLC water and acetonitrile in a ratio of 1 to 1 and a flow rate of 1 ml/min. The catalyst in the sample was removed by a strong magnet Tesla and a 0.22-micron PTFE injector filter. Subsequently, 2 ml of the catalyst was immediately placed in a container with 100 µl of 0.1 M sodium sulfite solution to remove ozone from the remaining solution. Afterwards, 20 µl of the sample was manually injected into the HPLC machine with a 100-µl Hamilton syringe. Standard concentrations of 0.2 ppm, 0.5 ppm, 0.8 ppm, 1 ppm, 5 ppm, 10 ppm, 20 ppm, and 30 ppm were injected into HPLC as standard. The calibration curve was obtained with R² = 0.9943. COD rate was measured by the colorimetric method at 400 nm with a 5000 Hach spectrophotometer (AHPHA 2015). Iron concentrations were measured by an atomic absorption apparatus

Results

The morphology and porosity of the internal structure of MNP are shown by scanning electron microscopy (FESEM) (Figure 2). Figure 3 represents the infrared FTIR spectroscopy analysis of MNP iron oxide nanoparticles. The observed peaks belong to the Fe-o group and are compatible with Fe₃O₄ synthesis.

Figure 4 shows the XRD pattern of the synthesized iron Nano oxide to determine the crystalline phase. As could be seen, all the obtained peaks can characterize the phase of pure iron oxide from iron oxide. No impurities were observed according to the XRD pattern. The mean crystal size (D) for MNP was calculated based on the Deby Scherrer $\theta \cos D = 0.99 \lambda / \beta$ equation, in which λ is equal to the X-ray wavelength (1.540598Å), β represents the full width and width at half maximum

scatter line expressed in radians, and θ represents the diffraction angle of the XRD spectrum. The mean crystal yield of MNP was about 40 nm, which confirms the results obtained from FESEM scanning electron microscopy analysis. Figure 5 illustrates BET Plot and Figure 6 represents t-Plot. The mean values of BET surface area,

pore size, and volume were $34.477 \text{ m}^2/\text{g}$, 2.4178 nm , and $0.3498 \text{ cm}^3/\text{g}$, respectively. The results showed that MNP had a mesoporous type structure. Figure 5 (a, b, and c) demonstrates the porosity, specific surface area, and model of the MNP nanoparticle isotherm.

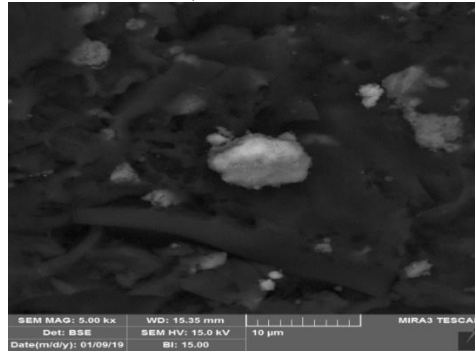


Figure.2- Appearance and properties of MNP ferrite nanoparticles.

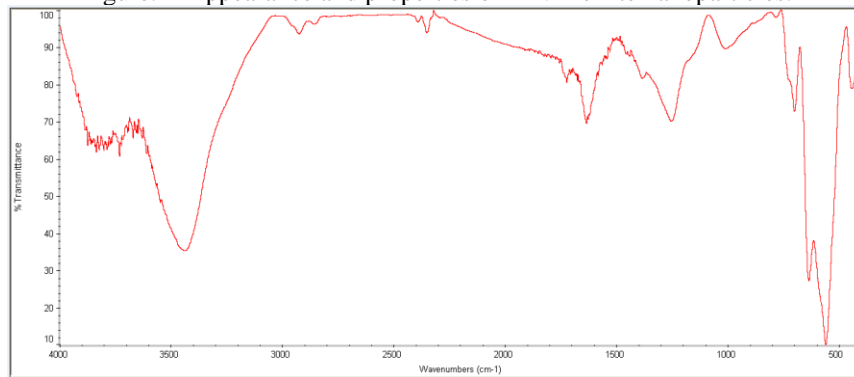


Figure.3- FTIR spectroscopic analysis.

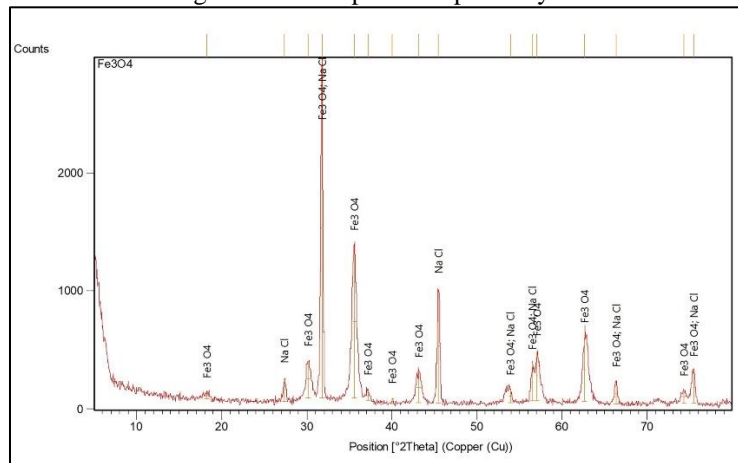


Figure.4- XRD spectrum of the synthesized Nanomagnet to determine the crystalline phase.

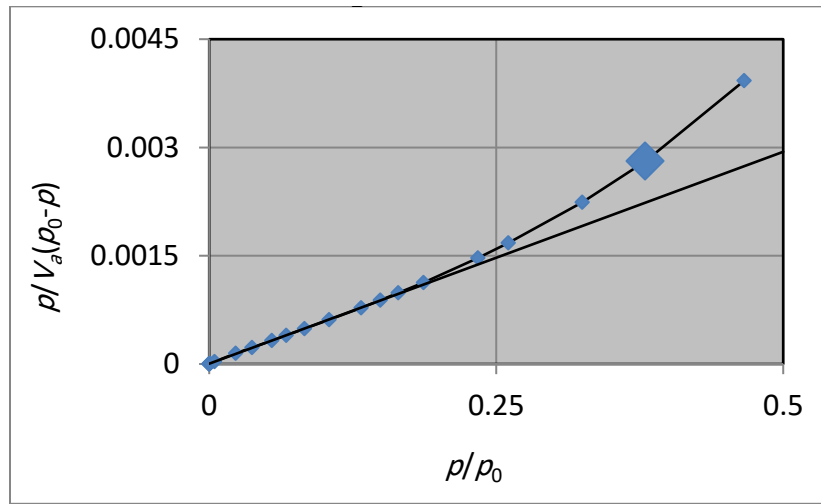


Figure.5- porosity (BET Plot).

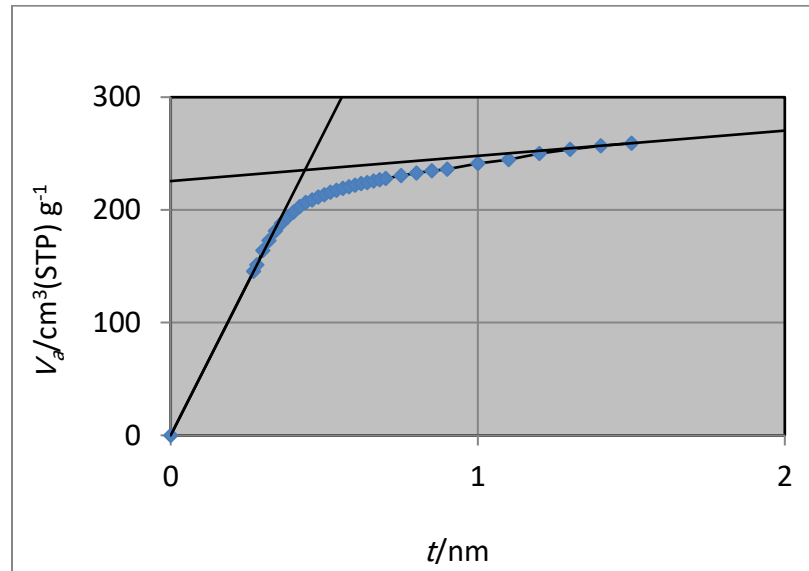


Figure.6- Specific surface area (t-Plot).

The present study investigated the effect pH in the range of 3 to 11 in the presence of magnetized nanoparticles of 0.1 g / l and the reaction time of 60 minutes (Figure 5). As could be seen, malathion degradation occurs more rapidly at the pH range of 3 to 5. These results were obtained from positively charged MNP-anionic form of malathion adsorbent in a pH acidic environment. The activated persulfate degraded malathion at the MNP level. On the other hand, with the increase in pH, malathion degradation decreased, which is due to the non-radical decomposition of persulfate in high acidity.

The results are presented in Figure 7. The highest efficiency belonged to the pH range of 3 to 5. In general, malathion decomposition efficiency was obtained at pHs of 3, 5, 7, 9, and 11 with 26, 24.4, 18, 8.8, and 6.8, respectively. In fact, in acidic and alkaline conditions, the efficiency of the process significantly reduced. Figures 6 and 7 show the effects of pH (pH = 3-5) and persulfate (with increasing dosage of persulfate to 2 mm) on malathion degradation. Malathion removal efficiency increased along with the catalyst dosage.

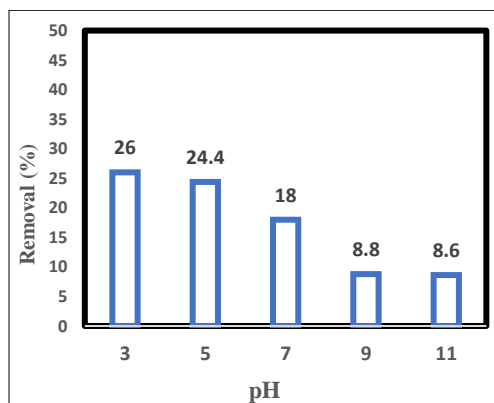


Figure.7- Effects of pH.

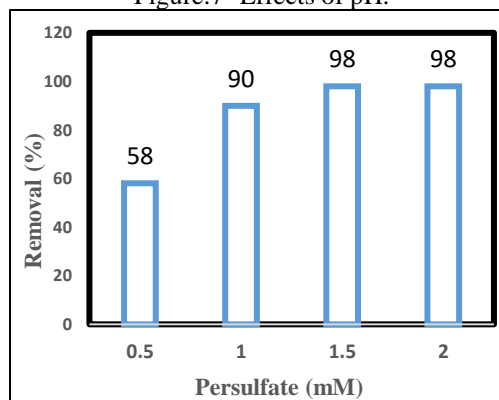


Figure.8- Effect of persulfate.

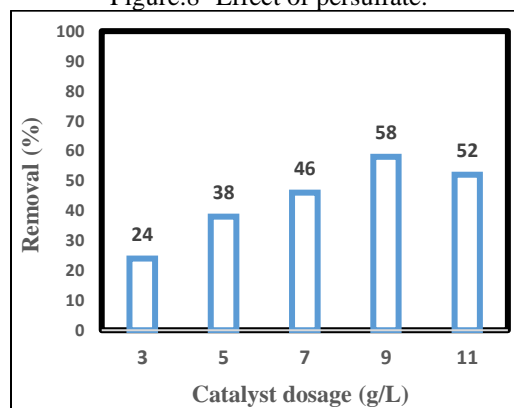


Figure.9- Catalyst dosage effect.

Figure 9 exhibits that malathion removal efficiency improves with increasing catalyst dosage. As shown, the use of persulfate alone is almost ineffective on the removal of malathion and its oxidative capacity is not sufficient to break down the malathion molecule and persulfate must be activated with organic compounds for degradation. Adding only 0.1 g / lit of iron nanoparticles could increase the system efficiency and improve catalyst removal efficiency. The increase in the catalyst efficiency and improvement in the system efficiency were found to be associated with the increase in the capacity and volume of iron at higher doses of iron nanoparticles (MNP) in the malathion removal process, which are 24, 38, 46, 58, and 52% for 0.1, 0.2, 0.3, 0.4, and 0.5 g / l MNP, respectively. The use of 0.5 g / l MNP did not show a significant change,

indicating the efficiency of the system with an increased dosage of MNP. Meanwhile, the rate of malathion degradation increased with the increase in the dosage of persulfate in a favorable trend. The removal of malathion for the amounts of persulfate was 58, 90, 98, and 98% for dosages of persulfate of 0.5, 1, 1.5, and 2 mM, respectively. As a result, the increased concentration of persulfate contributes to an increase in the amount of radical sulfate, which is effective on destroying malathion. This effect was observed in chemical oxidation processes, particularly in the Fenton process. Furthermore, the removal of malathion at the highest dosage of 2 mmol sulfate decreased slightly.

We studied malathion concentrations in the range of 1 to 100 mg / L with constant dosages of sulfate and

MNP. In Figure 10, the reduction in the rate of malathion degradation at higher concentrations could be attributed to the absence of sufficient free radicals for malathion degradation. It shows the rate of malathion degradation flow in concentrations (5 to 100 mg/lit) and with a constant dosage of 1.5 mM of persulfate and MNP; it also implies the rate of malathion degradation flow at higher concentrations. In a heterogeneous catalyst system at the nanoparticle level of iron, malathion degradation occurs

by sulfate radicals at active MNP sites. At high concentrations of malathion, a competitive reaction to adsorb malathion and active sulfate on the active MNP sites possibly occurs, which could limit the degradation of malathion; thus, the constant flow rate of malathion degradation by (persulfate / (Fe₃O₄)) / Fe₃O₄ @ CNT MNP / persulfate) was determined.

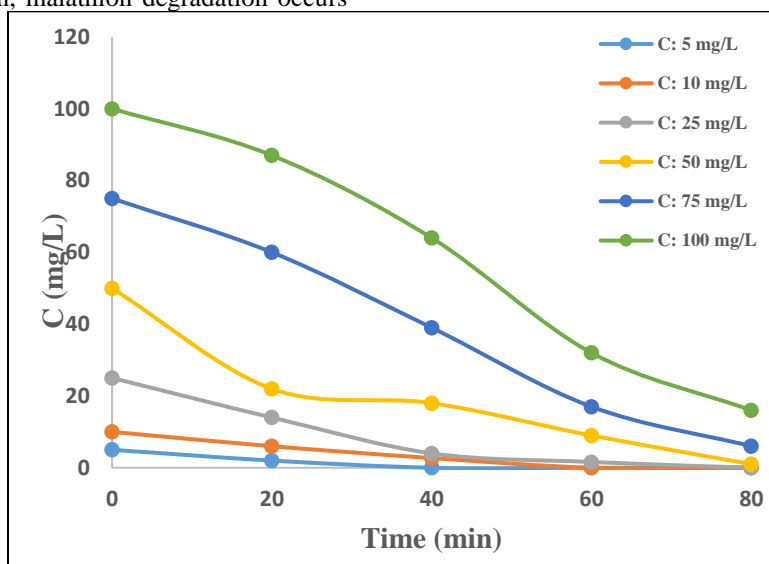


Figure.10- Flow rate trend of malathion degradation.

Figure 11 shows the removal of malathion in five consecutive stages. As observed, the efficiency and effectiveness of malathion removal gradually decreased over the five stages. The new catalyst indicated a removal efficiency of about 97%, which reached about 72% after

the fifth stage of malathion removal. On the other hand, catalyst surface contamination may be caused by the adsorption of organic and intermediate compounds, which leads to a decrease in catalytic activity (Qi et al., 2013).

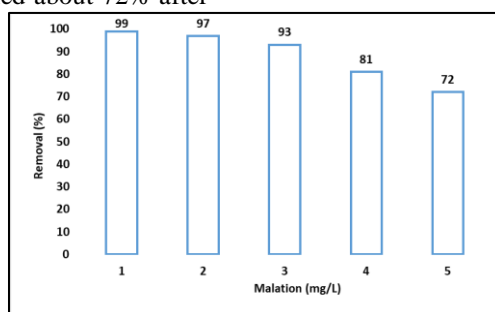


Figure.11- Elimination of malathion in five stages.

Conclusion

Pesticide pollution in aquatic environments is a serious chemical problem (Tsaboula, 2019). Iron oxide Nanoparticles are perfectly able to remove chemical materials (Kiani et al., 2019). The results of the present study revealed that the effectiveness of malathion removal from water using iron oxide nanoparticles (Fe₃O₄) depends on the concentration and pH parameters; hence, the removal efficiency showed a direct ratio with pH, yet an inversely proportional ratio with increased toxin concentration.

The results of this study are consistent with those of previous works. In the study by Phu et al. (2009), the

removal of arsenic using Iron oxide nanoparticles was affected by the pH of water. Adsorption of arsenic by nanoparticles was effective once pH was lower than 7 and reduced with the increase in pH. In the paper by Arjaghi et al. (2021), the ability to remove lead and cadmium by magnetic nanoparticles of iron oxide was respectively 82% and 77% for the initial concentration of 50 mg/l and a pH in the range of 5 to 4. The increase in the number of free radicals and ions due to the mechanisms of radiation is along with the increase in the input concentration of malathion toxin. Therefore, it is inferred that the free radicals produced in this process are in contact with more of the raw material and metabolites and as a result, the

efficiency of the process decreases with increasing concentration. In other words, when the duration of exposure to iron oxide nanoparticles (Fe_3O_4) is prolonged, a large number of free radicals are formed in the solution, which destroys malathion toxin as much as possible. In the study by Bahador et al. (2021), there was a reduction in adsorption once the concentration of heavy metals increased. In addition, Lin et al. (2018) showed that the optimum removal of cadmium affecting iron oxide nanoparticles is in low and moderate concentrations.

This study indicated that activated carbon modified with iron oxide nanoparticles is an effective adsorbent to remove malathion from water and effluents. About 82% of malathion was removed by loading iron oxide nanoparticles (Fe_3O_4) under the condition of pH = 5, PS = 1.5 Mm, MNP = 0.4 gr/L, in one hour. Iron nanoparticles (MNPs) performed better than homogeneous iron forms. The presence of chloride ions significantly reduced malathion degradation. The catalytic activity of iron nanoparticles for oxidants showed good performance. On the other hand, it improved the efficiency of the PS / MNP system in malathion degradation. However, the results of the present study are on a laboratory scale. It could be expected that the introduction of high amounts of nanoparticle oxide into aquatic environments have detrimental effects on aquatic health and aquatic ecosystems.

The real effects of nanotechnology must be determined and identified before the Nano waste appears in the environment and also prior to the introduction of new Nano products to the market. Proper management of these new compounds is suggested to prevent irreversible pollution and its toxic effects, as the green plants and algae are the first habitat in the nature, whose destruction will

References

- Arjaghi, S. K., Alasl, M. K., Sajjadi, N., Fataei, E., & Rajaei, G. E. (2021). Green Synthesis of Iron Oxide Nanoparticles by RS Lichen Extract and its Application in Removing Heavy Metals of Lead and Cadmium. *Biological trace element research*, 199(2), 763-768.
- Asghar, A., Raman, A. A. A., & Daud, W. M. A. W. (2015). Advanced oxidation processes for in-situ production of hydrogen peroxide/hydroxyl radical for textile wastewater treatment: a review. *Journal of cleaner production*, 87:826-838.
- Bacchetta, R., Santo, N., Marelli, M., Nosengo, G., & Tremolada, P. (2017). Chronic toxicity effects of ZnSO_4 and ZnO nanoparticles in *Daphnia magna*. *Environmental research*, 152:128-140.
- Bahador, F., Foroutan, R., Esmaili, H., & Ramavandi, B. (2021). Enhancement of the chromium removal behavior of *Moringa oleifera* activated carbon by chitosan and iron oxide nanoparticles from water. *Carbohydrate Polymers*, 251, 117085.

lead to the extinction of many living organisms in the continuation of the food chain. In general, the results of the current work relatively indicated that the physicochemical properties of nanoparticles, such as size, shape, surface, general morphology, and chemical composition, in different environmental conditions, can significantly affect carbon in removing malathion. In other words, the best conditions for the removal of malathion are obtained when the exposure time is long (60 minutes), the concentration is low (0.5 mg / l), and the pH is alkaline. Obviously, the use of chemical oxidation methods alone is not very popular today since it could be highly energy consuming and costly for water treatment processes. Therefore, to reduce the costs and energy consumption, it is preferred to utilize integrated methods of water and wastewater treatment in order to achieve the desired removal efficiency in short term and with the lowest energy consumption.

Grant Support Details

The present research did not receive any financial support.

Conflict of Interest

The authors declare that there is no conflict of interests regarding the publication of this manuscript. In addition, the ethical issues, including plagiarism, informed consent, misconduct, data fabrication and/or falsification, double publication and/or submission and redundancy has been completely observed by the authors.

Life Science Reporting

No life science threat was practiced in this research.

- Bownik, A. (2017). *Daphnia* swimming behaviour as a biomarker in toxicity assessment: a review. *Science of the total environment*, 601:194-205.
- Buchman, J. T., Bennett, E. A., Wang, C., Tamijani, A. A., Bennett, J. W., Hudson, B. G., ... & Haynes, C. L. (2020). Nickel enrichment of next-generation NMC nanomaterials alters material stability, causing unexpected dissolution behavior and observed toxicity to *S. oneidensis* MR-1 and *D. magna*. *Environmental Science: Nano*, 7(2):571-587.
- Deknock, A., De Troyer, N., Houbraken, M., Dominguez-Granda, L., Nolivos, I., Van Echelpoel, W., ... & Goethals, P. (2019). Distribution of agricultural pesticides in the freshwater environment of the Guayas river basin (Ecuador). *Science of the Total Environment*, 646, 996-1008.
- Edokpayi, J. N., Odiyo, J. O., & Durowoju, O. S. (2017). Impact of wastewater on surface water quality in developing countries: a case study of South Africa. *Water quality*, 401-416.
- Fataei, E., Seyyed Sharifi, Amir, Hasanpour Kourandeh, H., Seyyed Sharifi Amin, Safaviyan, ST., (2013) .

- Nitrate removal from drinking water in laboratory-scale using iron and sand nanoparticles, *Int J Biosci*, 3(10):256-261.
- Gajda-Meissner, Z., Matyja, K., Brown, D. M., Hartl, M. G., & Fernandes, T. F. (2020). Importance of Surface Coating to Accumulation Dynamics and Acute Toxicity of Copper Nanomaterials and Dissolved Copper in *Daphnia magna*. *Environmental toxicology and chemistry*, 39(2):287-299.
- Guan, Y. H., Ma, J., Ren, Y. M., Liu, Y. L., Xiao, J. Y., Lin, L. Q., & Zhang, C. (2013). Efficient degradation of atrazine by magnetic porous copper ferrite catalyzed peroxymonosulfate oxidation via the formation of hydroxyl and sulfate radicals. *Water research*, 47(14):5431-5438.
- Khalili Arjaghi, S., Ebrahimzadeh Rajaei, G., Sajjadi, N., Kashefi Alasl, M., & Fataei, E. (2020). Removal of Mercury and Arsenic Metal Pollutants from Water Using Iron Oxide Nanoparticles Synthesized from Lichen *Sinensis Ramalina* Extract. *Journal of Health*, 11(3), 397-408.
- Khan, K., Khan, P. M., Lavado, G., Valsecchi, C., Pasqualini, J., Baderna, D., ... & Benfenati, E. (2019b). QSAR modeling of *Daphnia magna* and fish toxicities of biocides using 2D descriptors. *Chemosphere*, 229:8-17.
- Kiani, M., Bagheri, S., & Karachi, N. (2019). Adsorption of purpurin dye from industrial wastewater using Mn-doped Fe₂O₄ nanoparticles loaded on activated carbon. *Desalination and Water Treatment*, 152, 366-373.
- Köck-Schulmeyer, M., Villagrasa, M., de Alda, M. L., Zhu, H., Han, J., Xiao, J. Q., & Jin, Y. (2013). Uptake, translocation, and accumulation of manufactured iron oxide nanoparticles by pumpkin plants. *Journal of Environmental monitoring*, 10(6):713-717.
- Li, C., Zhou, K., Qin, W., Tian, C., Qi, M., Yan, X., & Han, W. (2019). A review on heavy metals contamination in soil: effects, sources, and remediation techniques. *Soil and Sediment Contamination: An International Journal*, 28(4), 380-394.
- Lin, J., Su, B., Sun, M., Chen, B., & Chen, Z. (2018). Biosynthesized iron oxide nanoparticles used for optimized removal of cadmium with response surface methodology. *Science of the Total Environment*, 627, 314-321.
- Liu, X., Tian, J., Li, Y., Sun, N., Mi, S., Xie, Y., & Chen, Z. (2019). Enhanced dyes adsorption from wastewater via Fe₃O₄ nanoparticles functionalized activated carbon. *Journal of hazardous materials*, 373, 397-407.
- Mishra, M., & Chun, D. M. (2015). α -Fe₂O₃ as a photocatalytic material: A review. *Applied Catalysis A: General*, 498:126-141.
- Nogueira, D. J., Vaz, V. P., Neto, O. S., da Silva, M. L. N., Simioni, C., Ouriques, L. C., ... & Matias, W. G. (2020). Crystalline phase-dependent toxicity of aluminum oxide nanoparticles toward *Daphnia magna* and ecological risk assessment. *Environmental research*, 182:108987.
- Nowack, B. (2009). The behaviour and effects of nanoparticles in the environment. *Environmental pollution*, 157(4), 1063-1185.
- Olaniran, A. O., Singh, L., Kumar, A., Mokoena, P., & Pillay, B. (2017). Aerobic degradation of 2, 4-dichlorophenoxyacetic acid and other chlorophenols by *Pseudomonas* strains indigenous to contaminated soil in South Africa: Growth kinetics and degradation pathway. *Applied Biochemistry and Microbiology*, 53(2):209-216.
- Omrani, M., Fataei, E., (2018). Synthesizing Colloidal Zinc Oxide Nanoparticles for Effective Disinfection; Impact on the Inhibitory Growth of *Pseudomonas aeruginosa* on the Surface of an Infectious Unit, *Pol. J. Environ. Stud.*, 27:1639-1645.
- Qi, F., Chu, W., & Xu, B. (2013). Catalytic degradation of caffeine in aqueous solutions by cobalt-MCM41 activation of peroxymonosulfate. *Applied Catalysis B: Environmental*, 134:324-332.
- Paramo, L. A., Feregrino-Pérez, A. A., Guevara, R., Mendoza, S., & Esquivel, K. (2020). Nanoparticles in agroindustry: Applications, toxicity, challenges, and trends. *Nanomaterials*, 10(9), 1654.
- Peng, C., Zhang, W., Gao, H., Li, Y., Tong, X., Li, K., ... & Chen, Y. (2017). Behavior and potential impacts of metal-based engineered nanoparticles in aquatic environments. *Nanomaterials*, 7(1), 21.
- Phu, N. D., Phong, P. C., Chau, N., Luong, N. H., Hoang, L. H., & Hai, N. H. (2009). Arsenic removal from water by magnetic Fe_{1-x}Co_xFe₂O₄ and Fe_{1-y}Ni_yFe₂O₄ nanoparticles. *Journal of Experimental Nanoscience*, 4(3), 253-258.
- Rajaei, G. E., Khalili-Arjaghi, S., Fataei, E., Sajjadi, N., & Kashefi-Alasl, M. (2020). Fabrication and characterization of polymer-based nanocomposite membrane modified by magnetite nanoparticles for Cd²⁺ and Pb²⁺ removal from aqueous solutions. *Comptes Rendus. Chimie*, 23(9-10), 563-574.
- Rai, P. K., Kumar, V., Lee, S., Raza, N., Kim, K. H., Ok, Y. S., & Tsang, D. C. (2018). Nanoparticle-plant interaction: Implications in energy, environment, and agriculture. *Environment international*, 119, 1-19.
- Rezaei-Aghdam, E., Shamel, A., Khodadadi-Moghaddam, M., Rajaei, G. E., & Mohajeri, S. (2021). Synthesis of TiO₂ and ZnO Nanoparticles and CTAB-Stabilized Fe₃O₄ nanocomposite: kinetics and thermodynamics of adsorption. *Research on Chemical Intermediates*, 47(5), 1759-1774.
- Safarkar, R., Ebrahimzadeh Rajaei, G., & Khalili-Arjaghi, S. (2020). The study of antibacterial properties of iron oxide nanoparticles synthesized using the extract of lichen *Ramalina sinensis*. *Asian Journal of Nanosciences and Materials*, 3(3), 157-166.
- Saravanan, A., Kumar, P. S., Govarthan, M., George, C. S., Vaishnavi, S., Mouliswaran, B., ... & Yaashikaa,

- P. R. (2021). Adsorption characteristics of magnetic nanoparticles coated mixed fungal biomass for toxic Cr (VI) ions in aquatic environment. *Chemosphere*, 267, 129226.
- Sasani, M., Fataei, E., Safari R., Nasehi, F., Mosayebi, M., (2021) . Antimicrobial Potentials of Iron Oxide and Silver Nanoparticles Green-Synthesized in *Fusarium solani*, *Journal of Chemical Health Risk*, 10.22034/jchr.2021.1928198.1293.
- Schwarzenbach, R. P., Egli, T., Hofstetter, T. B., Von Gunten, U., & Wehrli, B. (2010). Global water pollution and human health. *Annual review of environment and resources*, 35, 109-136.
- Sengul, A. B., & Asmatulu, E. (2020). Toxicity of metal and metal oxide nanoparticles: A review. *Environmental Chemistry Letters*, 18(5), 1659-1683.
- Slater, T. J., Janssen, A., Camargo, P. H., Burke, M. G., Zaluzec, N. J., & Haigh, S. J. (2016). STEM-EDX tomography of bimetallic nanoparticles: A methodological investigation. *Ultramicroscopy*, 162, 61-73.
- Teja, A. S., & Koh, P. Y. (2009). Synthesis, properties, and applications of magnetic iron oxide nanoparticles. *Progress in crystal growth and characterization of materials*, 55(1-2), 22-45.
- Tony, A. M., El-Geundi, M. S., Hussein, S. M., & Abdelwahab, M. Z. (2017). Degradation of malathion in aqueous solutions using advanced oxidation processes and chemical oxidation. *Direct Research Journal of Agriculture and Food Science*, 5, 174-185.
- Tsaboula, A., Papadakis, E. N., Vryzas, Z., Kotopoulou, A., Kintzikoglou, K., & Papadopoulou-Mourkidou, E. (2019). Assessment and management of pesticide pollution at a river basin level part I: Aquatic ecotoxicological quality indices. *Science of The Total Environment*, 653, 1597-1611.
- Venkatesan, G., & Subramani, T. (2018). Environmental degradation due to the industrial wastewater discharge in Vellore District, Tamil Nadu, India.
- Vymazal, J., & Březinová, T. (2015). The use of constructed wetlands for removal of pesticides from agricultural runoff and drainage: a review. *Environment international*, 75:11-20.
- Zhang, F., Wang, Z., Song, L., Fang, H., & Wang, D. G. (2020). Aquatic toxicity of iron-oxide-doped microplastics to *Chlorella pyrenoidosa* and *Daphnia magna*. *Environmental Pollution*, 257:113451.
- Zhou, N., Zhang, Y., Nian, S., Li, W., Li, J., Cao, W., & Wu, Z. (2017). Synthesis and characterization of Zn1-xCoxO green pigments with low content cobalt oxide. *Journal of Alloys and Compounds*, 711:406-413.
- Zhu, L., Ai, Z., Ho, W., & Zhang, L. (2013). Core-shell Fe-Fe₂O₃ nanostructures as effective persulfate activator for degradation of methyl orange. *Separation and Purification Technology*, 108:159-165.